On-line monitoring of the freeze-drying process: A new image-based PAT.

Proceedings of Eurodrying'2019
Torino, Italy, July 10-12, 2019

Paper 77

On-line Monitoring of the Freeze-Drying Process: a new image-based PAT

Domenico Colucci*, *Davide Fissore

Dipartimento di Scienza Applicata e Tecnologia, Politecnico di Torino
Corso Duca degli Abruzzi 24, 10129, Torino, Italy
Email: domenico.colucci@polito.it

Abstract

In this work a Process Analytical Technology (PAT) for the on-line monitoring of a Vacuum Freeze-Drying (VFD) based on the information extracted from the infrared images of the process is presented and validated. An infrared camera, placed inside the drying chamber, provided information about the thermal evolution of the process over time; after images pretreatment and segmentation, temperature profiles were extracted and processed to obtain the variables of interest. Experiments were carried out according to factorial design on a set of different operating conditions, namely fluid temperature and chamber pressure, type of vials and solid percentage in the solution. Both sucrose and mannitol solutions, were studied. Together with the temperature in several positions along the product height, we were able to correctly estimate the ending time of the primary drying phase together with the sublimating interface position and the heat and mass transfer coefficients, K_v and R_p. Those two parameters have a dramatic importance since they can be used in a mathematical model of the process for on-line or off-line optimization of the process. Being based on a contactless technology, the PAT studied in this work does not present any issue regarding the sterility requirement of the process or the possible interference of the sensing element with the product dynamics.

***Keywords**: Infrared imaging; Lyophilization; Real time monitoring; Process analytical Technology*

1. Introduction

In recent years the number of drugs and pharmaceutical products that require a freeze-drying step in the manufacturing process, for solvent removal and drug stabilization, has increased, together with the challenges presented to the practitioners. Freeze-drying is particularly appreciated, compared to other drying processes, since the water content is reduced at low temperature via sublimation from a frozen product, thus avoiding any damage to thermolabile molecules. Trapped into a solid structure, the active compounds can be stored, also at room temperature, for long time. Furthermore, the highly porous and hydrophilic structure of the dried product can be easily rehydrated and reconstituted.

A typical freeze-drying cycle is composed of three stages, namely freezing, primary drying, and secondary drying. After the product has been poured into the vials, it is frozen, and the second stage of the process starts. The pressure in the chamber is reduced and the shelf temperature is raised to allow the sublimation of the ice. As the water vapor leaves the product, the ice front, the interface separating the frozen layer from the dried one, recedes from the top to the bottom of the product. In the secondary drying the bound water is removed to reach the desired value of residual moisture. This is achieved by increasing the temperature in the chamber; pressure does not have a real effect in this step (Pikal et al., 1990). The operation is typically a batch process, and the temperature of the fluid flowing inside the shelves and chamber pressure are the only variables that could be manipulated (Mellor, 1978; Jennings, 1999; Oetjen and Haseley, 2004; Costantino and Pikal 2004; Fissore, 2013).

The development of new Process Analytical Technologies (PAT) able to obtain information on the ongoing process that might be used for real time monitoring, control and optimization of the process is still a major concern in the field and has been strongly incentivized by the American Food and Drug Administration in the *Guidance for industry PAT* published in 2004. Fissore et al. (2018) reviewed the technologies proposed so far for process monitoring and control, comparing and discussing their pros and cons.

Primary drying is the most time demanding step of the vacuum freeze-drying process and, given the high amount of residual ice, the riskiest. In this phase an adequate Process Analytical Technology (PAT) should constantly monitor the temperature of the product and assure that the threshold for product denaturation, amorphous products collapse, or crystalline products melting, is not trespassed (Bellows and King, 1972; Tsourouflis et al., 1976). Another very important variable that must be monitored is the residual amount of solvent to avoid unnecessary extension of the process or that the temperature is raised, to start the secondary drying stage, when the ice is not completely sublimated, and the product quality could be jeopardized. Real time prediction of the parameters required by the mathematical models used, either in-line (Pisano et al., 2010; Pisano et al., 2011a) or off-line (Giordano et al., 2010; Fissore et al., 2011), for model control and optimization is also valuable. The two main parameters that are required for online estimation are K_v and R_p, respectively the heat and mass transfer coefficients used to model the heat flow from the shelf to the product and the water vapor mass flow from the interface of sublimation to the drying chamber (Velardi and Barresi, 2008).

The direct measurement of the temperature of the product was proven to be an effective strategy for monitoring and control of the VFD process (Fissore et al., 2017). Besides using multiple temperature measurements, it is also possible to model and account for the *in-batch* variability typical of the process (Bosca et al., 2013). The main limit to this approach is that usually a thermocouple, at lab-scale, or thermistors, preferred for industrial applications since they are more robust and could be sterilized, has to be inserted inside the vial and this could interfere with the drying kinetics of the process. Furthermore, the presence of electronics and wires does not fit the requirements of the pharmaceutical industries in terms of automatization (i.e. loading, stoppering and discharge) and sterility.

Emteborg et al. (2014) firstly proposed to use an infrared camera to measure the temperature of the product. In their work the camera was mounted on the ceiling of a freeze-dryer, where a window of germanium guarantees the field of view inside the chamber: the camera is protected from the harsh characteristics of a freeze-drying chamber, namely low temperature, low pressure and moisture reach environment, but it just allows to look the first shelf from the top. Van Bockstall et al. (2018) placed the camera outside the drying chamber and used the online thermal measurements to monitor and optimize a continuous spin freeze-drying process. Lietta et al. (2019) presented and validated a sensor placed inside the drying chamber: it is based on an infrared camera, enclosed into a case designed to protect the electronics from the surroundings, thus enabling the use of this sensor in existing equipment, without any retrofit, and in any shelf and position inside the chamber. In this work, after validation of the temperature measurements the effectiveness of this technology in estimating both K_v and R_p was proven. Besides this kind of sensor was proved to shield the vial in front of it from the effects of radiation from the chamber wall, providing for these vials a measurement that is representative of the state of most of the batch.

The algorithm presented in this paper extracts the axial thermal profile of the vial, the position of the sublimation interface, H_i, from which the amount of residual ice and the water mass flow can be estimated, its temperature, T_i, and an estimation of the ending time of the process. A large set of experiment was carried out to validate the accuracy of these measurements and estimates under different conditions. Besides, for each condition tested, K_v and R_p were estimated and proved to abide by the physics of the system.

Section 2 introduces the experimental setup, the details about the design of experiment (DoE) performed and the algorithm used to pretreat and extract the information from the IR images. Section 3 presents the main results and section 4 the general conclusions of the work.

2. Materials and methods

The drying experiments were carried out in a lab scale equipment, LyoBeta 25™ freeze-dryer (Telstar, Spain), having a chamber volume of 0.2 m^3, a total shelf area of 0.5 m^2 and a capacity of the external ice condenser of 40 kg. The sensor described by Lietta et al. (2019) was used to monitor the thermal evolution of the product. It consists of an infrared and an RGB camera housed, together with all the electronics, inside a plastic material case. The material, Ertacetal C, and design of this case allow both positioning the sensor inside the drying chamber and the wi-fi communication with the exterior. In all tests ten vials (ISO 8362-1) were placed at 30 cm from the sensor, and 500 images were acquired at five minutes from each other during the primary drying stage.

Five variables were tested at two levels but only half of the combinations were considered according to 2^{5-1} DoE; Figure 1 reports a graphical representation of the conditions tested. The five variables considered are: i) shelf temperature: -10 °C and -30°C, ii) the pressure in the chamber: 10 Pa and 20 Pa, iii) kind of sugar: sucrose and mannitol, iv) the solid percentage in the solution: 5% b.w. and 10% b.w. and v) the kind of vial: 4R and 10R.

The thermal images obtained are 256x320 pixels. Before their analysis they were always corrected for the *barrel effect* induced by the lens (De Villiers et al., 2008) and registered to compensate the movements of the vials and of the sensor due to the vibrations of the equipment (Gonzalez et al., 2004).

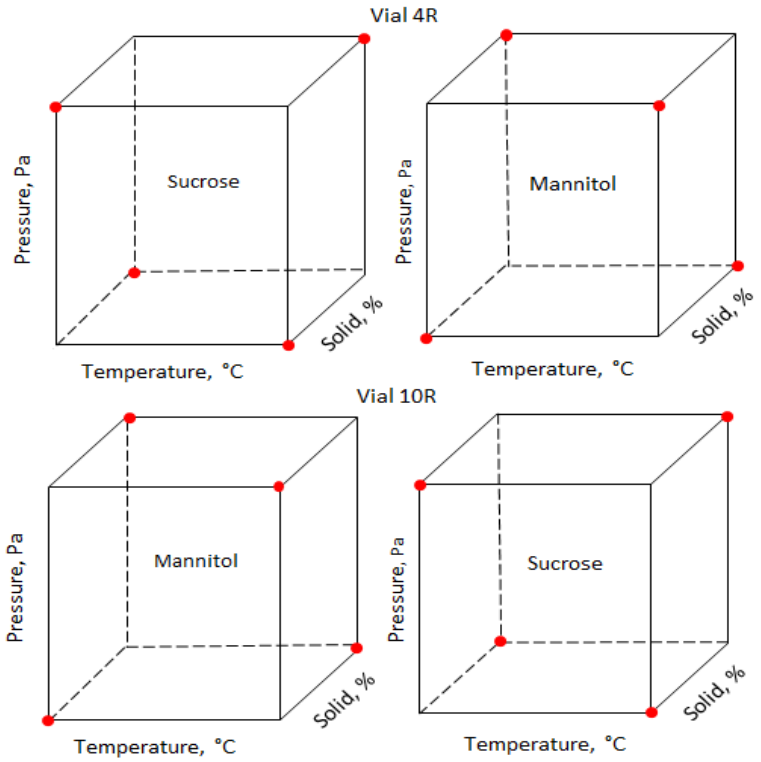

Figure 1. Graphical representation of the 2^{5-1} factorial Design of Experiment used for this work. Red dots represent the conditions actually tested.

For every image acquired from the sensor an algorithm automatically pretreats the images and acquires the temperature axial profiles in three different positions for every vial. The three thermal profiles obtained for a single vial were averaged to filter the noise of the measurement and, then, the local minimum was identified. The pixel corresponding to this minimum identifies the position of the sublimation interface, H_i; its temperature is T_i.

K_v and R_p were obtained directly from the values of the H_i, T_i, T_b, the temperature at the bottom of the vial also extracted from the aforementioned axial profile, and T_f, the temperature of the heating fluid flowing inside the shelves, according to Equation (1) and (2):

$$K_v = \frac{k_{eff}\left(\frac{T_f - T_i}{T_f - T_b} - 1\right)}{L - H(t)} \tag{1}$$

$$R_p = \frac{\Delta H_s \left(p_{w,i}(T_i) - p_{w,c}\right)}{K_v \left(T_{sh} - T_b\right)} \tag{2}$$

where ΔH_s is latent heat of sublimation, k_{eff} the thermal conductivity of the frozen layer and p_w the water vapor partial pressure at the interface (subscript *i*) and inside the drying chamber (subscript *c*) respectively. Equation (1) was obtained from a heat balance at the frozen layer, while Equation (2) from an energy balance at the sublimation interface, under the assumption that, at the interface, all the heat provided is used for sublimation (Velardi and Barresi, 2008). A multiway ANOVA was performed to look for the variables having a significant effect (p-value lower than a given threshold, in this work we used 0.1) on the parameters.

3. Results and discussion

Figure 2 reports an example of the trajectories of H_i and T_i obtained using the algorithm presented. H_i is reported as dimensionless value with respect to the actual height of the product L:

$$H_i = \frac{z_i}{L} \tag{3}$$

where z_i is the actual position of the interface in millimeters.

The position of the sublimation interface decreases slower during the first hour of the drying, then the slope changes and the ice front retreats linearly until a value of 0.05 is reached around 9 hours; almost the same time is the *onset*, the time the Pirani-Baratron ratio starts changing its slope. In all our experiments, after the freezing, we first decreased the pressure to the set point and, then, the temperature of the shelf was raised. In this first transitory the temperature of the frozen product slightly increases, and, the corresponding vapor pressure at the ice front might slightly overcome the partial water vapor pressure in the chamber. This driving force justifies the slow sublimation rate in this first period. When the fluid temperature raises the driving force, sublimation is enhanced and the sublimation rate increases. H_i then slowly decreases until it reaches a constant value of zero at 18 h. The noise of the measurement increases again at 25 h, a time almost corresponding to the *offset* the second slope change of the Pirani-Baratron ratio. When all the ice has been removed the product goes to the equilibrium, there is not a real minimum anymore in the temperature profile and the algorithm might pick up some local minima due to the noise of the signal.

The temperature of the ice front suddenly increases of more than 10 degrees within the first one hour and a half of drying, then slows down until a value of -15°C is reached after 7 more hours. This trend agrees with what we observed about H_i. Sublimation starts as soon as the pressure in the chamber is reduced below the partial pressure of the water vapor; then, when we start supplying heat, the frozen product heats up, raising the vapor pressure at the ice front and enhancing the sublimation rate. Ice sublimation is endothermic and, thus, when the shelf temperature reaches the set point, an equilibrium is stablished between the two phenomena. When the resistance to mass transport, that depends on the height of the dried layer, becomes too high, the product starts heating again: this explains why the temperature increases again after 10 h, when both the Pirani over Baratron ratio and H_i change their slope. T_i increases for 15 additional hours, with a constantly increasing slope, until reaching a constant value around 25 h from the beginning of the primary drying stage. The product has reached the thermal equilibrium with the environment, there is no more water vapor flow and the Pirani gauge measures the same pressure of the Baratron manometer. We could expect primary drying to be completely over when the ice front reaches the bottom of the vial, but this is not the case.

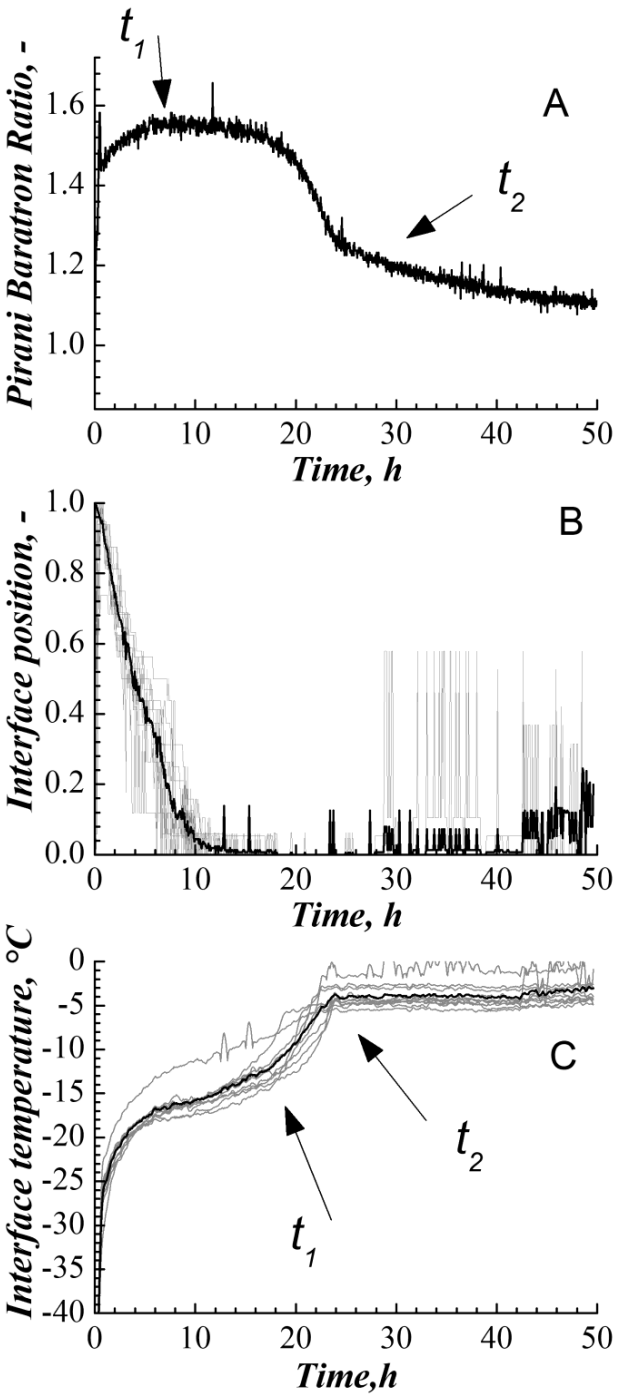

Figure 2. A: Pirani-Baratron ratio. B: Interface position, H_i for each one of the vials of the same batch (gray lines) and average profile (black line). C: Temperature of the sublimating front, T_i for each one of the vials of the same batch (gray lines) and average profile (black line). Ten 10R vials filled with 5 ml of a 5% b.w. D-mannitol solution. Shelf temperature: -10°C; chamber pressure: 10Pa

The more reasonable explanation to this apparent nonsense is that the product is a cylinder and we are monitoring its external surface. The heat transfer inside the product is not perfectly uniform. Especially when only ten vials are set in the middle of a shelf, radiation from the surroundings plays a dramatic role and the sublimating area is not planar, but it has a curvature towards the vial wall. The sublimation front reaches the bottom of the vial earlier where it is more exposed to additional heat flux and later in the center of the cake. In this time lapse, the minimum temperature read by the algorithm is always at the bottom of the vial, but its temperature keeps raising since the sublimation of the ice in the inner core of the product cannot completely counteract the heat provided by the thermal fluid.

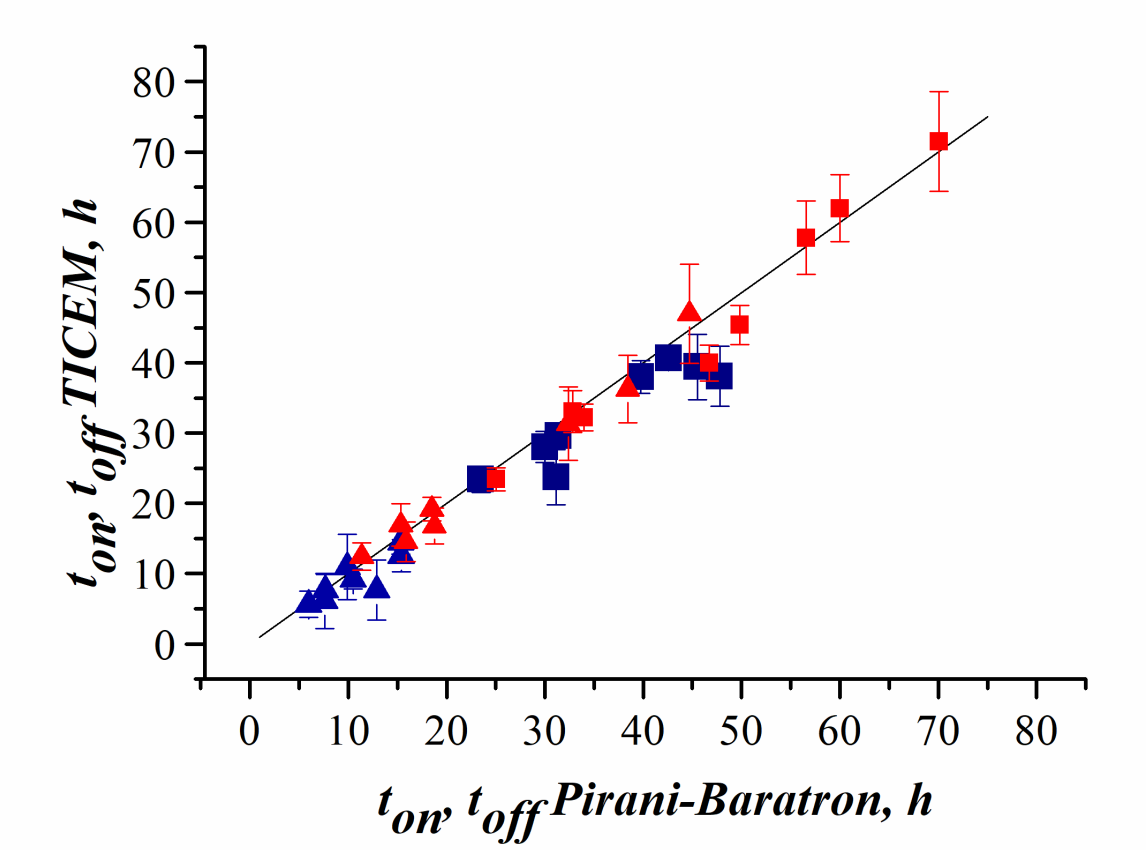

Figure 3. parity plot of the onset (triangles) and offset (squares) for the different experimental conditions. Sucrose solution (blue), mannitol solution (red).

The measured values of the onset (t_{on}) and offset (t_{off}) time obtained from the Pirani over Baratron pressure ratio (Patel et al., 2010) of the process was compared to the estimations obtained from the actual trajectory of T_i for each one of the conditions tested. In these thermal profiles, Figure 2, the *onset* corresponds to a clearly visible slope change while, at the offset, the temperature profile becomes mostly constant, showing that the thermal equilibrium has been reached inside the product.

The parity plot reported in Figure 3 shows a good agreement between the two measurements of the ending point of the primary drying. Our algorithm appears to constantly slightly underestimate the *offset* of the sucrose solutions, probably because the temperature profile approaches the asymptotic value in a less marked way and, in such a highly noisy signal the definition of the exact moment the temperature goes asymptotic cannot be so precise.

K_v and R_p can be directly estimated from the measurements extracted from the thermal images. K_v was found to increase with temperature, Figure 4A, and increase with pressure, Figure 4B. Both the effects of temperature and pressure were proved to be statistically significant (p-value < 0.1). As expected, the heat transfer coefficient is independent (p-value > 0.1) of the kind of sugar and the

amount of solid in the solution, Figure 4C and Figure 4D (Pisano et al., 2011b). A moderate dependency of K_v from the shape and geometry of the vials was obtained but the large variability in the measurements made it not statistically significant (not shown). R_p was found dependent on the kind of sugar and its content in the solution (p-value < 0.1) only.

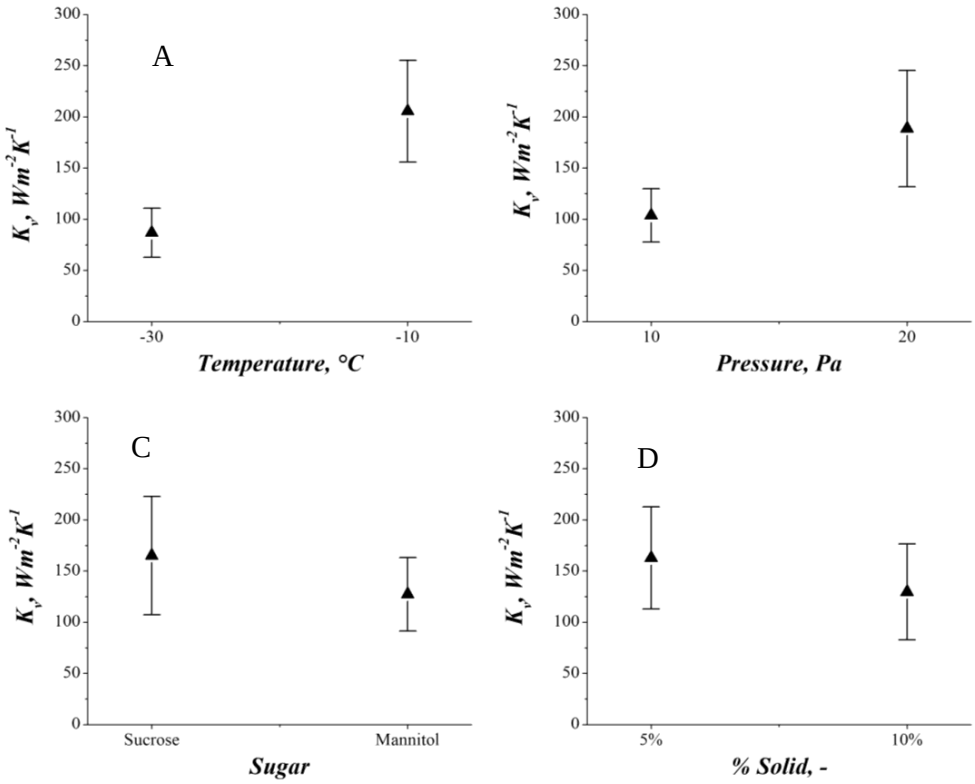

Figure 4. Experimentally obtained values of the heat transfer coefficient as a function of temperature (A), pressure (B) and amount of solid in the solution (C).

4. Conclusions

Infrared imaging was presented in the past years as an effective technology for real time monitoring of the vacuum freeze-drying process. In this paper we deepened the possible outcomes of this approach.

At first, we presented the possibility to extract, directly from the thermal images, both the position of the sublimation front, that is an estimation of the residual amount of ice inside the product, and its temperature, the most critical one, given that at the sublimation interface the relatively high amount of water could still jeopardize the product quality. From the evolution of the temperature at the interface we can also determine the ending point of the primary drying stage. The maximum temperature inside the product can be monitored to make sure it always lay beneath the desired threshold. This technology and the algorithm here presented could effectively detect any deviation of the batch from its target evolution, allowing a quick response and the correction of the operating conditions before the product is impaired.

Together with the temperature and position of the ice front also the temperature measured at the bottom of the vial can be extracted from the axial profile. These three measurements, together with the temperature of the heating fluid, can be used to estimate the kinetic parameters used to model the process. The quality of the inferred estimation was proved by verifying the agreement of the obtained values with the physics of the system. The estimation in real time of these parameters can be used for real time and/or off-line optimization and control of the process.

Future work will aim to apply the methodology here presented to the on-line monitoring and control of the freezing stage, and to couple the information extracted from the infrared camera with that of the RGB camera already embedded inside the system.

References

Bellows, R.J., King, C.J.,1972, Freeze-drying of aqueous solutions: Maximum allowable temperature. *Cryobiology* **9**(6), 559-561.

Bosca, S., Corbellini, S., Barresi, A.A., Fissore, D., 2013, Freeze-drying monitoring using a new process analiytical technology: toward a "zero defect" process. *Drying Technol.* **31**(15), 1744-1755.

Costantino, H.R., Pikal, M.J. 2004, Lyophilization of Biopharmaceuticals, AAPS Press: Arlington, VA.

De Villiers, J.P., Leuschner, F.W., Geldenhuys, R. (2008), Centi-pixel accurate real-time inverse distortion correction. *Proc. SPIE*, Vol. 7266, pp. 11-1-11-8.

Emteborg, H., Zeleny, R., Charoud-Got, J., Martos, G., Luddeke, J., Schellin, H., Teipel, K., 2014, Infrared thermography for monitoring of freeze-drying processes: instrumental developments and preliminary results. *J. Pharm. Sci.* **103**, 2088-2097.

Fissore, D., Pisano, R., Barresi, A. A., 2011, Advanced Approach to Build the Design Space for the Primary Drying of a Pharmaceutical Freeze-Drying Process. *J. Pharm. Sci.* **100**(11), 4922–4933.

Fissore, D. 2013, Freeze-drying of pharmaceuticals, in: *"Encyclopedia of Pharmaceutical Science and Technology"* (Swarbrick J, Ed.), 4th Edition. CRC Press, London, UK, pp. 1723-1737.

Fissore, D., Pisano, R., Barresi, A., 2017, On the use of temperature measurement to monitor a freeze-drying process for pharmaceuticals. *I2MTC 2017 - Proc. IEEE International Instrumentation and Measurement Technology Conference*, Torino, Italy, 22-25 May, pp. 1276-1281.

Fissore, D., Pisano, R., Barresi, A.A., 2018, Process analytical technology for monitoring pharmaceutical freeze-drying – A comprehensive review. *Drying Technol.* **36**(15), 1839-1865.

Giordano, A., Barresi A.A., Fissore, D., 2010, On the use of mathematical models to build the design space for the primary drying phase of a pharmaceutical lyophilization process, *J. Pharm. Sci.* **100**(1), 311-324.

Gonzalez, R.C., Woods, R.E., Eddins, S.L., 2004, Digital image processing using Matlab. Pearson education, Inc., Upper Saddle River, New Jersey.

Jennings, T.A., 1999, Lyophilization: introduction and basic principles. Interpharm/CRC Press, Boca Raton.

Lietta E., Colucci D., Distefano G., Fissore, D., 2019, On the use of IR thermography for monitoring a vial freeze-drying process. *J. Pharm. Sci.* **108**, 391-398.

Mellor, J.D., 1978, Fundamentals of freeze-drying. Academic Press, London.

Oetjen, G.W., Haseley P., 2004, Freeze-Drying. Wiley-VHC. Weinheim.

Patel, S.M., Doen, T., Pikal, M.J., 2010, Determination of the end point of primary drying in freeze-drying process control. *AAPS PharmSciTech* **11**(1), 73-84.

Pikal, M.J., Shah, S., Roy, M.L., Putman, R., 1990, The secondary drying stage of freeze drying: drying kinetics as a function of temperature and chamber pressure. *J. Pharm. Sci.* **60**(3), 203-207.

Pisano, R., Fissore, D., Velardi, S. A., Barresi, A. A., 2010, In-Line Optimization and Control of An Industrial Freeze-Drying Process for Pharmaceuticals. *J. Pharm. Sci.* **99**(11), 4691–4709.

Pisano, R., Fissore, D., Barresi, A. A., 2011a, Freeze-Drying Cycle Optimization using Model Predictive Control Techniques. *Ind. Eng. Chem. Res.* **50**(12), 1920 7363–7379.

Pisano R., Fissore D., Barresi A., 2011b, Heat transfer in freeze-drying apparatus, in: *"Developments in Heat Transfer"* (Dos Santos Bernardes, Ed.), Chap. 6, InTechOpen, Croazia: pp. 91-114.

Tsourouflis, S., Flink, J.M., Karel, M.,1976, Loss of structure in freeze-dried carbohydrates solutions: effect of temperature, moisture content and composition. *J. Sci. Food Agric.* **27**(6), 509-519.

U. S. Department of Health and Human Services, Food and Drug Administration, Center for Drug Evaluation and Research (CDER), Center for Veterinary, Medicine (CVM), Office of Regulatory Affairs (ORA), Pharmaceutical CGMPs. (2004), Guidance for Industry, PAT A Framework for Innovative Pharmaceutical Development, Manufacturing, and Quality Assurance. https://www.fda.gov/downloads/drugs/guidances/ucm070305.pdf (last access date: April 2019).

Van Bockstal, P.J., Corver, J., De Meyer, L., Vervaet, C., De Beer, T., 2018, Thermal imaging as a noncontact inline process analytical tool for product temperature monitoring during continuous freeze-drying of unit doses. Anal. Chem. **90**(22), 13591-13599.

Velardi S.A., Barresi A.A., 2008, Development of simplified models for the freeze-drying process and investigation of the optimal operating conditions, *Chem. Eng. Res. Des.* **86**, 9-22.